Towards High Efficiency CO$_2$ Utilization by Glow Discharge Plasma

Stephan Renninger *, Paul Rößner, Jan Stein, Maike Lambarth and Kai Peter Birke

Electrical Energy Storage Systems, Institute for Photovoltaics, University of Stuttgart, Pfaffenwaldring 47, 70569 Stuttgart, Germany; paul.roessner@ipv.uni-stuttgart.de (P.R.); jan.stein@ipv.uni-stuttgart.de (J.S.); maike.lambarth@ipv.uni-stuttgart.de (M.L.); peter.birke@ipv.uni-stuttgart.de (K.P.B.)

* Correspondence: stephan.renninger@ipv.uni-stuttgart.de; Tel.: +49-711-6856-1508

Abstract: Plasma technology reaches rapidly increasing efficiency in catalytic applications. One such application is the splitting reaction of CO$_2$ to oxygen and carbon monoxide. This reaction could be a cornerstone of power-to-X processes that utilize electricity to produce value-added compounds such as chemicals and fuels. However, it poses problems in practice due to its highly endothermal nature and challenging selectivity. In this communication a glow discharge plasma reactor is presented that achieves high energy efficiency in the CO$_2$ splitting reaction. To achieve this, a magnetic field is used to increase the discharge volume. Combined with laminar gas flow, this leads to even energy distribution in the working gas. Thus, the reactor achieves very high energy efficiency of up to 45% while also reaching high CO$_2$ conversion efficiency. These results are briefly explained and then compared to other plasma technologies. Lastly, cutting edge energy efficiencies of competing technologies such as CO$_2$ electrolysis are discussed in comparison.

Keywords: plasma catalysis; CO$_2$ splitting; glow discharge; energy efficiency; CO$_2$ electrolysis; CO$_2$ utilization; magnetic field; power-to-X

1. Introduction

Many fields offer solutions for CO$_2$ utilization. Among them are thermochemical processes, electrolysis [1] and plasma catalysis; the latter has the smallest technology readiness level (TRL) but also offers a large potential for future improvements [2–4]. Attention is focused mostly on four types of plasma reactors: dielectric barrier discharges (DBDs) [5], gliding arc (GA) [6,7], atmospheric pressure glow discharges (APGD) [8,9] and microwave (MW) plasmas [10,11]. Increasing their energy efficiency and conversion at ambient pressure is the main point of concern. We recently presented reactors using a direct current APGD, which delivered promising results [12]. To further improve the previous design, it was scaled and now uses a laminar gas flow instead of a turbulent one. To be used industrially, a plasma reactor should operate at ambient pressure. However, this makes it hard to maintain a stable discharge. Two major difficulties are the negative differential resistance [13] and glow-to-arc transition [14]. A discharge thus tends to form a narrow, low-resistance arc that can damage the plasma source and is not useful in catalysis. To suppress these effects, current control strategies or vortex gas flow [14] are often used in recent studies to disperse the plasma [8]. The reactor setup presented here uses a magnetic field instead to force the plasma into a large disc-like volume. This approach is viable for various discharge forms, such as gliding arc plasma reactors [15,16]. A laminar gas flow can be then used to introduce energy into the working gas as homogeneously as possible. This communication aims to give an update on the ongoing design process for an improved plasma reactor for the CO$_2$ splitting reaction.

2. Materials and Methods

The reactor vessel was a glass tube with an inner diameter of 38 mm. Direct current formed a discharge between two copper electrodes. One was an axial rod, the other a ring. CO_2 was introduced into the reactor through an injection plate with 22 axial nozzles in concentric nozzles, arranged in concentric circles. The injector was placed 120 mm above the plane of the electrodes. An axial magnetic field was provided by permanent magnets below the electrode assembly, and the field strength was 30 mT on the central axis. A packed bed made from zirconia balls was placed 2 mm below the discharge plane inside the ring electrode. It serves to suppress thermal currents in the gas and could also help with quenching the hot exhaust gas. Zirconia was chosen because it is chemically inert, non-conductive and can be used to carry catalysts in future experiments. The reactor assembly is shown in Figure 1. The input gas flow V_{in} consisted of pure CO_2. It was measured by an analogue rotameter and adjusted using a needle valve. The assembly was calibrated using a displacement cylinder. The exhaust gas was characterized using non-dispersive infrared sensors (SmartGas Flow Evo; Heilbronn; Germany); measurements at a flow of V_{in} =1.4 SLM were confirmed by a gas chromatographer (Trace 1310 Thermo Scientific; Waltham, MA, USA). The sensors were placed 1 m downstream from the reactor in the exhaust gas pipe. Power was provided to the electrodes by a custom current-limiting driver circuit. It delivers direct current for ignition (up to 25 kV) and is sustaining of the discharge (<2 kV). Mean burn voltage of the discharge and mean current were measured. Mean values are deemed sufficient here, because a large choke inductor of 1.5 H was placed on the output of the driver circuit, leading to low current ripple. Voltage ripple was typically around 15%. The discharge power P_d was calculated from the power supplied to the driver circuit by a lab power supply and the known driver efficiency. To confirm these values, they can also be calculated as the product of burn voltage and current. CO_2 conversion X is calculated using Equation (1), while energy efficiency η is calculated by Equation (2). They use the concentrations of CO and CO_2 in the exhaust gas. ΔH_r = 12.6 J SCC^{-1} (standard cubic centimeter) is the reaction enthalpy of the CO_2 splitting reaction. Measurements of the gas concentrations were taken after a steady state in exhaust gas concentrations occurred.

$$X = \frac{c_{CO,out}}{c_{CO,out} + c_{CO2,out}} \tag{1}$$

$$\eta = \frac{X \, \Delta H_r \, \dot{V}_{in}}{P_{el}} \tag{2}$$
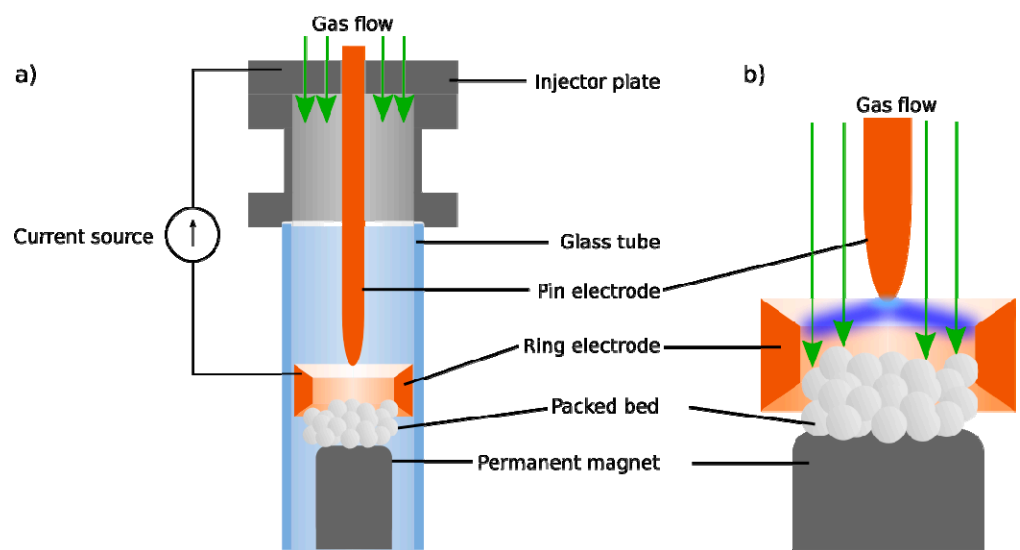
Figure 1. Overview over the plasma reactor assembly (**a**) and schematic view of the discharge (**b**).

3. Results

The achieved CO_2 conversion X and energy efficiency η for different discharge power P_d and gas flow rates V_{in} is shown in Figure 2. The highest conversion X was achieved at a discharge power of P_d = 165 W. The best energy efficiency η that was achieved is 45% at the highest gas flow rate of 1.25 SLM. The effectiveness of the magnetic field could be determined visibly: the discharge rotates quickly, so it gives the appearance of a disk to the naked eye. This leads to very homogeneous energy input into the gas. Quantizing the influence of the magnetic field will be the subject of future experiments.
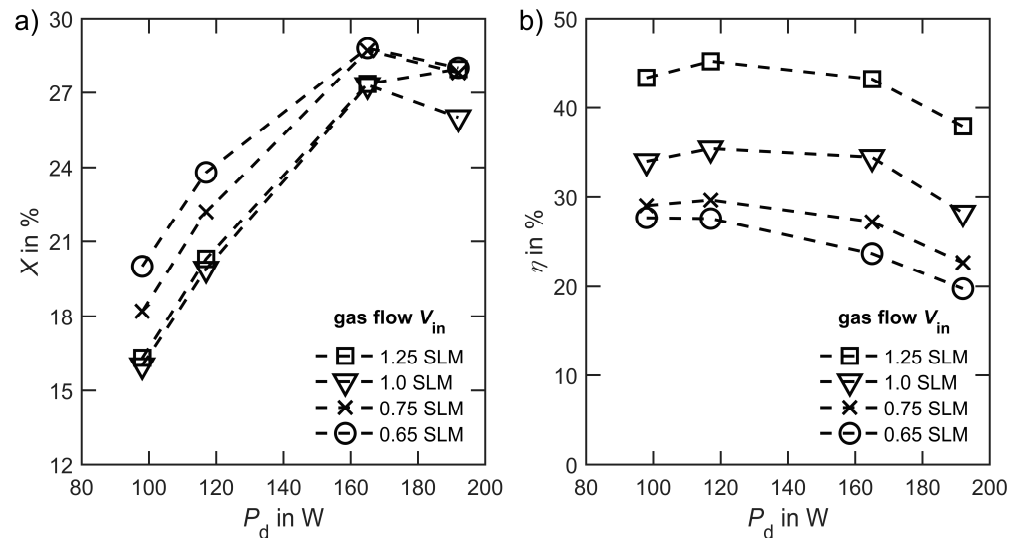
Figure 2. Performance of the reactor at different gas flow rates V_{in} and discharge power P_d. In (**a**), the conversion X is shown while (**b**) displays energy efficiency η.

4. Discussion

4.1. Performance of the Reactor

Conversion depends strongly on discharge power P_d. One reason is that higher power equals higher specific energy input. Additionally, the properties of the plasma, such as temperature, electron density and reduced electric field, can also be expected to change with the discharge power. In this reactor the rotation of the discharge filament accelerates at higher discharge powers. This can also be expected to have a positive influence on the conversion, since the gas will be swept more efficiently by the plasma. However, the conversion does not increase with power indefinitely. At the highest discharge power of P_d = 192W, conversion reduces. One reason could be the heating of the packed bed. This heating reduces the quenching rate, which increases the rate of the recombination reaction, thus again forming CO_2 [11]. Energy efficiency seems to mainly depend on gas flow rate but also decreases at high discharge powers.

4.2. Comparison to Other Technologies

The results achieved compare well to other plasma-based systems, as shown in Figure 3a. They were selected based on performance from a broader range of systems previously reviewed [17], considering more recent work. Gliding arcs provide high efficiency at ambient pressure; a vortex is often used to increase the discharge volume [6,7]. Gliding arcs also obtain good results without vortex flow [18]. Glow discharges can also benefit from vortex gas flow [8]. Increasing their stability is possible by operation in non-self-sustaining mode [9]. DBDs that moderate efficiency and conversion could be boosted by using a burst mode, where high power density is applied intermittently [5]. Microwave plasmas reach the most promising results to date [10]. However, these were obtained at very low pressures, and at ambient pressures even after utilizing precise quenching, efficiency is lower, yet still impressive [11]. The highest efficiencies reported in literature were achieved

at a very low pressure by radio frequency excitation at a pressure of just 40 Pa [19]. A common theme in the results seems to be that a homogeneous energy input into the gas results in good performance. Vortex gas flow as used in [6–8] can distribute energy well but is ultimately a chaotic process that will not lead to even energy distribution. In contrast, the combination of laminar flow and a disk-like discharge can distribute energy very evenly.
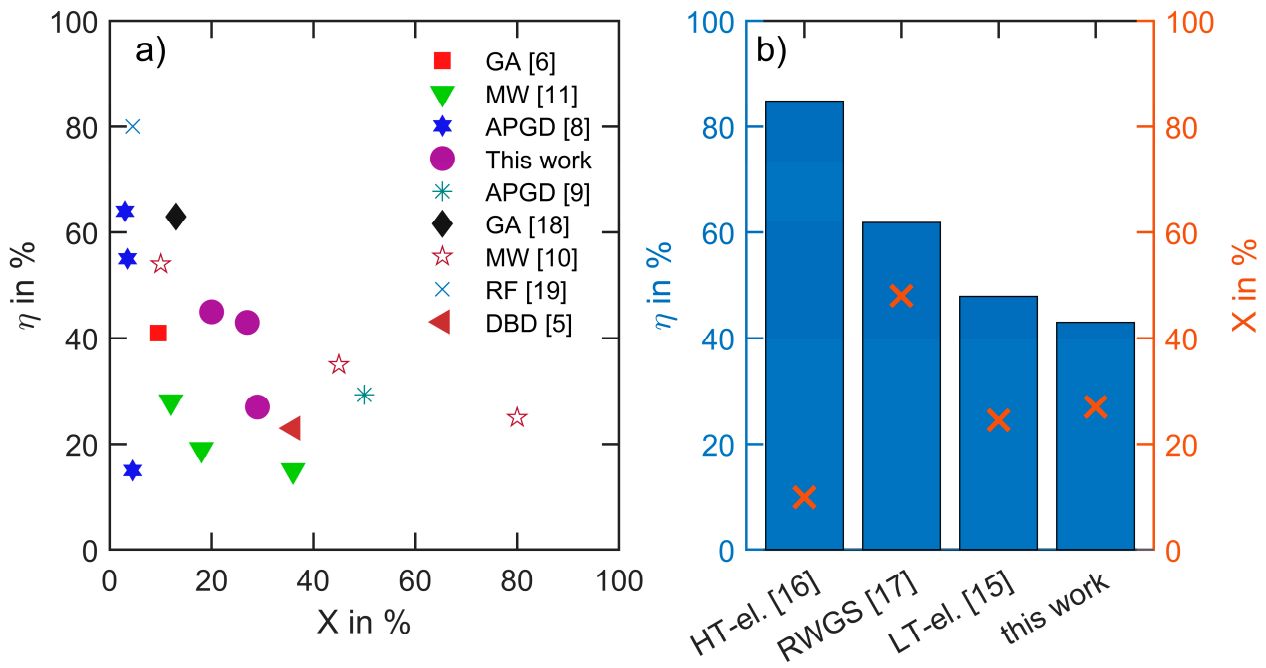
Figure 3. A comparison of the achieved energy efficiency η and conversion X for CO_2 splitting by plasma is shown in (**a**). In (**b**) the results are compared to high temperature electrolysis (HT-el.), low temperature electrolysis (LT-el.) and reverse water gas shift (RWGS).

In the following, a quantitative assessment of different CO_2 conversion technologies regarding energy efficiency η is given. The comparison has no claim for completeness and focuses only on the actual conversion step of CO_2 to CO; influences on a systemic level or scaling effects are not included here. This approach allows a comparison of vastly different technologies but is not intended as a ranking given that each technology has its own ideal configuration in which the full potential can be realized. Figure 3b shows calculated energy efficiencies drawn from recent publications (see Appendix A for the calculation). The technologies included are low temperature, gas-phase CO_2 electrolysis [20], high temperature CO_2 electrolysis in a solid oxide electrolysis cell [21], a thermochemical approach (Reverse Water Gas Shift, RWGS) [22] and the plasma approach reported in this work. The energy efficiencies given in Figure 3b show that each technology has the potential to enable a reasonable application. This is reasoned on the basis that systemic effects of the individual application have the potential to outweigh the differences inherent to the energy efficiency of the CO_2 conversion.

5. Conclusions

The presented glow discharge plasma reactor achieves a competitive CO_2 conversion of 27% and energy efficiency of 42%. This is a respectable performance since the process was running at ambient pressure. We attribute this good performance to the efficient sweeping of the gas by the discharge due to the magnetic field. In general, the energy efficiency of plasma-based systems is gaining ground compared to competing technologies such as electrolysis and thermochemical approaches. Focus thus shifts to scalability, lifespan and, most importantly, integration. After all, none of the presented technologies manage to produce pure product gases; their separation is a major task for which few technologies

are available. The integration of electrochemical oxygen pumps or separation membranes into plasma reactor systems will be a future focus. Our results illustrate that plasma technology can play an important role in CO_2 utilization, which is a cornerstone of a fossil-free economy.

Author Contributions: Conceptualization, S.R., J.S. and P.R.; methodology, S.R; investigation, S.R., M.L. and J.S.; resources, K.P.B.; writing—original draft preparation, S.R.; writing—review and editing, P.R. and M.L.; visualization, S.R.; supervision, K.P.B.; project administration, M.L.; funding acquisition, K.P.B. All authors have read and agreed to the published version of the manuscript.

Funding: This work was funded by the Federal Ministry for Economic Affairs and Energy (Germany) in the scope of their initiative "Energy transition in the transport sector" and the associated "PlasmaFuel" project (Funding code: 03EIV161A).

Informed Consent Statement: Not applicable.

Data Availability Statement: The data is not filed into a public repository but will be kindly provided upon request.

Conflicts of Interest: The authors declare no conflict of interest.

Appendix A

The energy efficiency of electrolysis is calculated considering electrical E_{el} and thermal energy E_{th} input following Equation (A1). Thermal energy is calculated by using the heat capacity c_p and temperature difference from ambient ΔT. Electrical energy is calculated using the Faradaic efficiency η_F, cell voltage U_{cell} at a current density of 200 mA cm^{-2}, electron number z and the Faraday constant F.

$$\eta = \frac{E_{use}}{E_{th} + E_{el}} = \frac{\Delta H_r^0}{c_p \Delta T + U_{cell} \eta_{FE}\, zF} \tag{A1}$$

For the thermochemical approach, energy input is the sum of thermal energy used for gas heating and utilized hydrogen. Hydrogen was weighed as an energy expense of $E_{H2} = 350$ kJ mol^{-1}.

References

1. Saravanan, A.; Kumar, P.S.; Vo, D.-V.N.; Jeevanantham, S.; Bhuvaneswari, V.; Narayanan, V.A.; Yaashikaa, P.; Swetha, S.; Reshma, B. A comprehensive review on different approaches for CO_2 utilization and conversion pathways. *Chem. Eng. Sci.* **2021**, *236*, 116515. [CrossRef]
2. Bogaerts, A.; Centi, G. Plasma technology for CO_2 conversion: A personal perspective on prospects and gaps. *Front. Energy Res.* **2020**, *8*, 111. [CrossRef]
3. Bogaerts, A.; Tu, X.; Whitehead, J.C.; Centi, G.; Lefferts, L.; Guaitella, O.; Azzolina-Jurry, F.; Kim, H.-H.; Murphy, A.B.; Schneider, W.F. The 2020 plasma catalysis roadmap. *J. Phys. D Appl. Phys.* **2020**, *53.44*, 443001. [CrossRef]
4. Grim, R.G.; Huang, Z.; Guarnieri, M.T.; Ferrell, J.R.; Tao, L.; Schaidle, J.A. Transforming the carbon economy: Challenges and opportunities in the convergence of low-cost electricity and reductive CO_2 utilization. *Energy Environ. Sci.* **2019**, *13*, 472–494. [CrossRef]
5. Ozkan, A.; Dufour, T.; Silva, T.; Britun, N.; Snyders, R.; Reniers, F.; Bogaerts, A. DBD in burst mode: Solution for more efficient CO_2 conversion? *Plasma Sources Sci. Technol.* **2016**, *25*, 055005. [CrossRef]
6. Trenchev, G.; Bogaerts, A. Dual-vortex plasmatron: A novel plasma source for CO_2 conversion. *J. CO_2 Util.* **2020**, *39*, 101152. [CrossRef]
7. Ramakers, M.; Medrano, J.A.; Trenchev, G.; Gallucci, F.; Bogaerts, A. Revealing the arc dynamics in a gliding arc plasmatron: A better insight to improve CO_2 conversion. *Plasma Sources Sci. Technol.* **2017**, *26*, 125002. [CrossRef]
8. Bharathi, R.; Sarathi, R.; Vinu, R. Development of a Swirl-Induced Rotating Glow Discharge Reactor for CO_2 Conversion: Fluid Dynamics and Discharge Dynamics Studies. *Energy Technol.* **2020**, *8.12*, 2000535.
9. Andreev, S.; Zakharov, V.; Ochkin, V.; Savinov, S. Plasma-chemical CO_2 decomposition in a non-self-sustained discharge with a controlled electronic component of plasma. *Spectrochim. Acta Part A Mol. Biomol. Spectrosc.* **2004**, *60*, 3361–3369. [CrossRef]
10. Bongers, W.; Bouwmeester, H.J.; Wolf, B.; Peeters, F.; Welzel, S.; Bekerom, D.V.D.; Harder, N.D.; Goede, A.; Graswinckel, M.; Groen, P.W.; et al. Plasma-driven dissociation of CO_2 for fuel synthesis. *Plasma Process. Polym.* **2016**, *14*, e1600126. [CrossRef]

11. Kim, H.; Song, S.; Tom, C.P.; Xie, F. Carbon dioxide conversion in an atmospheric pressure microwave plasma reactor: Improving efficiencies by enhancing afterglow quenching. *J. CO₂ Util.* **2019**, *37*, 240–247. [CrossRef]

12. Renninger, S.; Lambarth, M.; Birke, K.P. High efficiency CO_2-splitting in atmospheric pressure glow discharge. *J. CO₂ Util.* **2020**, *42*, 101322. [CrossRef]

13. Saifutdinov, A.I.; Timerkaev, B.A. Features of Transient Processes in DC Microdischarges in Molecular Gases: From a Glow Discharge to an Arc Discharge with a Unfree or Free Cathode Regime. *JETP Lett.* **2020**, *112*, 405–412. [CrossRef]

14. Rabinovich, A.; Nirenberg, G.; Kocagoz, S.; Surace, M.; Sales, C.; Fridman, A. Scaling Up of Non-Thermal Gliding Arc Plasma Systems for Industrial Applications. *Plasma Chem. Plasma Process.* **2021**, 1–16. [CrossRef]

15. Li, L.; Zhang, H.; Li, X.; Huang, J.; Kong, X.; Xu, R.; Tu, X. Magnetically enhanced gliding arc discharge for CO_2 activation. *J. CO₂ Util.* **2019**, *35*, 28–37. [CrossRef]

16. Zhang, H.; Li, L.; Li, X.; Wang, W.; Yan, J.; Tu, X. Warm plasma activation of CO_2 in a rotating gliding arc discharge reactor. *J. CO₂ Util.* **2018**, *27*, 472–479. [CrossRef]

17. Snoeckx, R.; Bogaerts, A. Plasma technology—A novel solution for CO_2 conversion? *Chem. Soc. Rev.* **2017**, *46.19*, 5805–5863. [CrossRef] [PubMed]

18. Kim, S.C.; Lim, M.S.; Chun, Y.N. Reduction Characteristics of Carbon Dioxide Using a Plasmatron. *Plasma Chem. Plasma Process.* **2013**, *34*, 125–143. [CrossRef]

19. Spencer, L.F.; Gallimore, A.D. Efficiency of CO_2 Dissociation in a Radio-Frequency Discharge. *Plasma Chem. Plasma Process.* **2010**, *31*, 79–89. [CrossRef]

20. Liu, Z.; Yang, H.; Kutz, R.; Masel, R.I. CO_2 Electrolysis to CO and O_2 at High Selectivity, Stability and Efficiency Using Sustainion Membranes. *J. Electrochem. Soc.* **2018**, *165*, J3371–J3377. [CrossRef]

21. Kaur, G.; Kulkarni, A.P.; Giddey, S. CO_2 reduction in a solid oxide electrolysis cell with a ceramic composite cathode: Effect of load and thermal cycling. *Int. J. Hydrogen Energy* **2018**, *43*, 21769–21776. [CrossRef]

22. Zonetti, C.P.; Letichevsky, S.; Gaspar, A.B.; Sousa-Aguiar, E.F.; Appel, L.G. The NixCe0.75Zr0.25−xO2 solid solution and the RWGS. *Appl. Catal. A Gen.* **2014**, *475*, 48–54. [CrossRef]